JOURNAL OF VIROLOGY, Oct. 2008, p. 9717–9729 Vol. 82, No. 19
0022-538X/08/$08.00+0 doi:10.1128/JVI.00782-08

Cytopathogenicity of Classical Swine Fever Virus Correlates with Attenuation in the Natural Host[▽]

Andreas Gallei,[1] Sandra Blome,[2] Stefanie Gilgenbach,[1,2] Norbert Tautz,[3] Volker Moennig,[2] and Paul Becher[1,2]*

Institut für Virologie, Justus Liebig Universität Gießen, Frankfurter Straße 107, D-35392 Giessen, Germany[1]; Institut für Virologie, Stiftung Tierärztliche Hochschule Hannover, Bünteweg 17, D-30559 Hannover, Germany[2]; and Institut für Medizinische Molekularbiologie, Universität zu Lübeck, Ratzeburger Allee 160, D-23538 Lübeck, Germany[3]

Received 11 April 2008/Accepted 12 July 2008

For the important livestock pathogens classical swine fever virus (CSFV) and bovine viral diarrhea virus (BVDV), cytopathogenic (cp) and non-cp viruses are distinguished according to the induction of apoptosis in infected tissue culture cells. However, it is currently unknown whether cp CSFV differs from non-cp CSFV with regard to virulence in the acutely infected host. In this study, we generated helper virus-independent CSFV Alfort-Jiv, which encompasses sequences encoding domain Jiv-90 of cellular J-domain protein interacting with viral protein (Jiv). Expanding the knowledge of BVDV, our results suggest that Jiv acts as a regulating cofactor for the nonstructural (NS) protein NS2 autoprotease of CSFV and initiates NS2-3 cleavage in *trans*. For Alfort-Jiv, the resulting expression of large amounts of NS3 correlated with increased viral RNA synthesis and viral cytopathogenicity. Moreover, both cp Alfort-Jiv and the parental non-cp CSFV strain Alfort-p447 efficiently replicate in cell culture. Animal experiments demonstrated that in contrast to parental non-cp Alfort-p447, infection with cp Alfort-Jiv did not cause disease in pigs but induced high levels of neutralizing antibodies, thus elucidating that cp CSFV is highly attenuated in its natural host. In contrast to virulent Alfort-p447, the attenuated CSFV strain Alfort-Jiv induces the expression of cellular Mx protein in porcine PK-15 cells. Accordingly, the remarkable difference between cp and non-cp CSFV with regard to the ability to cause classical swine fever in pigs correlates with different effects of cp and non-cp CSFV on cellular antiviral defense mechanisms.

Pestiviruses are important livestock pathogens that belong to the family *Flaviviridae*, which also comprises the closely related human *Hepatitis C virus* as well as flaviviruses like *Yellow fever virus* and *West Nile virus* (32). The genus *Pestivirus* includes the species *Bovine viral diarrhea virus 1* (BVDV-1), BVDV-2, *Border disease virus* (BDV), *Classical swine fever virus* (CSFV), the tentative species *Giraffe virus*, as well as several additional unassigned viruses from wild ruminants (15). CSFV causes classical swine fever (CSF), one of the economically most important diseases in pigs worldwide. Pestiviruses are small enveloped particles encompassing a single-stranded RNA genome of positive polarity with a length of about 12.3 kb. The viral genomic RNA is neither capped nor polyadenylated and contains one large open reading frame (ORF) flanked by 5′ and 3′ nontranslated regions (NTRs), which harbor *cis*-active elements essential for viral translation and replication. The ORF encodes a polyprotein of approximately 3,900 amino acids (aa) that is co- and posttranslationally processed by cellular and viral proteases to the mature viral proteins (32, 44, 52, 73).

For pestiviruses, cytopathogenic (cp) and non-cp strains are distinguished by their ability to cause a cytopathic effect (CPE) in susceptible cell cultures (28, 43). The majority of pestiviruses isolated from their hosts are non-cp. With the exception of rare, highly virulent non-cp BVDV-2 strains causing severe disease including a hemorrhagic syndrome in cattle, acute infections with non-cp BVDV and BDV strains usually result in only mild or no clinical symptoms in nongestating cattle and small ruminants. For CSFV, highly virulent strains causing CSF with high mortality in pigs as well as moderate- and low-virulence strains have frequently been described.

The biological significance and molecular aspects of viral cytopathogenicity have been extensively studied for BVDV. It is well known that cp BVDV strains evolve mostly by nonhomologous RNA recombination in animals persistently infected with non-cp BVDV and comprise various genomic alterations including insertions of cellular mRNA sequences as well as duplications and deletions of viral sequences (e.g., see references 6, 9, 10, 12, 47, 49, and 72). Unlike non-cp BVDV, the cytopathogenicity of cp BVDV correlates with the efficient release of nonstructural (NS) protein NS3 at late phases of infection. The emergence of cp BVDV in persistently infected animals is crucial for the induction of lethal mucosal disease in cattle (17, 18). However, acute infections of naive, not persistently infected animals with cp BVDV strains do not cause such disease and usually result in no or only mild symptoms of disease.

In contrast to BVDV, cp CSFV strains were rarely identified (22, 29, 41, 75). Interestingly, all cp CSFV field isolates analyzed so far consist of a non-cp CSFV helper virus together with a cp viral subgenome that lacks the genomic region encoding the structural proteins as well as the NS proteins N^{pro}, p7, and NS2 (2, 36, 51). In addition, several studies reported on the generation of helper virus-independent (HVI) cp CSFV.

* Corresponding author. Mailing address. Institute of Virology, Department of Infectious Diseases, University of Veterinary Medicine, Bünteweg 17, D-30559 Hannover, Germany. Phone: 49 511 953-7160. Fax: 49 511 953-8898. E-mail: paul.becher@tiho-hannover.de.

▽ Published ahead of print on 23 July 2008.

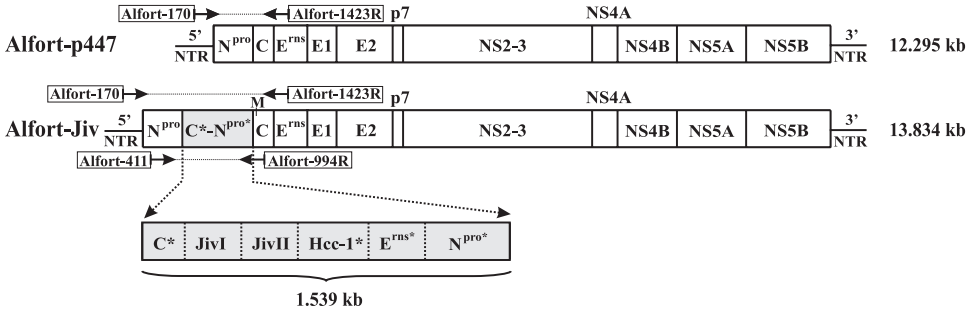

FIG. 1. Genome organizations of CSFV Alfort-Jiv and parental non-cp CSFV Alfort-p447. (Top) RNA genome of Alfort-p447 containing one large ORF (box) flanked by 5′ and 3′ NTRs. The positions of the genes encoding the viral structural proteins (capsid protein C and envelope proteins E^{rns}, E1, and E2) and NS proteins N^{pro}, p7, NS2-3, NS4A, NS4B, NS5A, and NS5B are indicated. (Bottom) Genome organization of Alfort-Jiv containing an insertion of 1.539 kb (C*-N^{pro}*) between the N^{pro} and C genes of Alfort-p447. C*-N^{pro}* is derived from cp BVDV strain CP8 and encodes a 513-aa fusion peptide encompassing fragments from viral sequences (C*, E^{rns}*, and N^{pro}*) and cellular sequences (JivI, JivII, and bovine homologue to human nuclear protein Hcc-1 [Hcc-1*]) (55). The lengths of the bars are not drawn to scale. Positions of primers used for RT-PCR analyses to investigate the genetic stability of Alfort-Jiv are indicated above (Fig. 3B) and below (Fig. 3C) the genomes, respectively. M, silently mutated first codon of C, a genetic marker for Alfort-Jiv. The sizes of Alfort-p447 and Alfort-Jiv are indicated in kilobases (kb) on the right.

However, either the respective virus strains were not genetically stable (27) or their cytopathogenicity was limited to certain virus-cell line combinations (4, 34, 48, 67). So far, nothing is known about the virulence of HVI cp CSFV inducing a CPE on different standard cell lines.

In the present study, we generated HVI cp CSFV Alfort-Jiv by introducing sequences encoding domain Jiv-90 of cellular J-domain protein interacting with viral protein (Jiv) between the N^{pro} and capsid genes of non-cp CSFV Alfort-p447. Analyses in tissue culture cells demonstrated that the cytopathogenicity of Alfort-Jiv correlated with efficient NS2-3 cleavage and the expression of large amounts of NS3, suggesting that Jiv-90 activates the CSFV autoprotease NS2 in *trans*. Animal experiments elucidated that in contrast to parental non-cp CSFV Alfort-p447, cp CSFV Alfort-Jiv is highly attenuated in its natural host. Finally, analysis of expression of the Mx protein in infected porcine PK-15 cells revealed that the difference in virulence between non-cp and cp CSFV correlates with the ability or inability to counteract cellular antiviral defense.

MATERIALS AND METHODS

Cells and viruses. Swine kidney (SK-6) cells were a kind gift of J. D. Tratschin, Institute of Virology and Immunoprophylaxis, Mittelhäusern, Switzerland. Porcine kidney Rie 5-1 cells were obtained from the Collection of Cell Lines in Veterinary Medicine (Friedrich Loeffler Institute, Isle of Riems, Germany). Madin-Darby bovine kidney (MDBK) and porcine kidney PK-15 cells were obtained from the American Type Culture Collection (Rockville, MD). Cells were grown in Dulbecco's modified Eagle's medium supplemented with 10% horse serum (MDBK and SK-6 cells) or fetal calf serum (Rie 5-1 and PK-15 cells). Cells were tested regularly for the absence of pestiviruses by reverse transcription (RT)-PCR and immunofluorescence (IF) (see below). Non-cp CSFV Alfort-p447 and cp CSFV Alfort-Jiv were derived from the infectious cDNA clones pAlfort-p447 (27) and pAlfort-Jiv (see below).

Construction of cDNA clone pAlfort-Jiv. Nucleotide numbers throughout this study refer to the sequence of Alfort-p447 (27). To generate cDNA clone 1, plasmid pAlfort-p447 (27) was first digested with AatII (positions 6463 and 12261) and religated into 8.5-kb plasmid pAlfort-p447ΔAatII. Subsequently, an additional SmaI site was introduced into pAlfort-p447ΔAatII at position 5145 by QuikChange PCR using primers QC-Alfort-SmaI-5145 and QC-Alfort-SmaI-5145R. Finally, the resulting plasmid was religated into 7.1-kb cDNA clone 1 after SmaI (position 5145)/SmaI (positions 12 and 295) digestion. cDNA clones 2 to 4 were generated by cloning specific PCR products 2 to 4 into vector p-GEM-T (Promega, Madison, WI). For PCR 2, pAlfort-p447 served as a template, and oligonucleotides Alfort-T7-NotI-1 and Alfort-BsmbI-NproR were used. In consequence, cDNA clone 2 contains an NheI site followed by a T7 RNA transcription promoter and pAlfort-p447-derived cDNA sequences that correspond to the viral 5′ NTR, the complete autoprotease N^{pro} gene, and the first 4 nucleotides (nt) of the capsid gene that are followed by a reversed and complementary BsmBI site. cDNA clone 3 was generated by use of oligonucleotides CP8-BsmBI-C* and CP8-BsmBI-Npro*R. Here, cDNA clone 12 (55) containing cp BVDV CP8-derived sequences served as a template. The resulting cDNA clone 3 contained a BsmBI site followed by the last 2 nt of the pAlfort-p447 N^{pro} gene, the complete CP8-derived C*-N^{pro}* insertion (with the last nucleotide silently mutated from C to T) (Fig. 1) (55), the first 4 nt of the pAlfort-p447 capsid gene (of which the first codon was silently mutated from TCC to AGC), and a reversed and complementary BsmBI site. Note that in contrast to the previously reported C*-N^{pro}* sequence (55), codon 37 of JivI is GTG instead of GCG, thus resulting in a deduced amino acid change from A to V. For PCR 4, pAlfort-p447 served as a template, and oligonucleotides Alfort-BsmBI-C and CST-57 were used. The resulting cDNA clone 4 contains a BsmBI site, which is followed by pAlfort-p447-derived sequences including the last 2 nt of the pAlfort-p447 N^{pro} gene (of which the last nucleotide was silently changed from C to T), the complete capsid gene, and most of the glycoprotein E^{rns} gene. Note that the first codon of the capsid gene was silently mutated from TCC to AGC; this serine codon serves as a genetic marker for Alfort-Jiv (Fig. 1). The cDNA sequences of clones 1 to 4 were controlled by nucleotide sequencing. Subsequently, cDNA clones 1 to 4 were digested with NotI/SbfI (position 1516) (clone 1), NotI/BsmBI (clone 2), BsmBI/BsmBI (clone 3), and BsmBI/SbfI (clone 4), respectively, and the four resulting cDNA fragments of about 5.6 kb (clone 1), 0.9 kb (clone 2), 1.5 kb (clone 3), and 0.6 kb (clone 4) were directly ligated into 8.6-kb cDNA clone 5. Finally, for the construction of infectious full-length cDNA clone pAlfort-Jiv, the cDNA clone 5-derived NotI/SbfI fragment of about 3.1 kb was introduced into pAlfort-p447 precut with NotI/SbfI. Further details on cloning procedures and sequences of the oligonucleotides used are available on request.

In vitro synthesis of RNA. After the complete digestion of plasmids pAlfort-p447 and pAlfort-Jiv with SmaI, linearized DNA was extracted with phenol-chloroform and precipitated with ethanol. RNA was transcribed by use of T7 (Ambion, Austin, TX) DNA-dependent RNA polymerase using standard conditions. The quality and amount of RNAs were controlled by ethidium bromide staining after agarose gel electrophoresis. RNA transcripts used for transfection contained >80% of intact RNA.

Transfection of synthetic viral RNA. For transfection, the confluent SK-6 cells from a dish that is 10 cm in diameter were treated with trypsin, resuspended in 0.4 ml of phosphate-buffered saline without Ca^{2+} and Mg^{2+}, and mixed with about 2 μg of in vitro-transcribed viral RNA immediately before the pulse (950 μF and 180 V). For electroporation, a Gene Pulser II (Bio-Rad, Munich, Germany) apparatus was used.

Infection of cells, crystal violet staining of cells, and determination of growth kinetics. Supernatants of transfected or infected cells were used for further infections. Material for infections was harvested 48 to 72 h postinfection (p.i.)

and stored at −70°C. Crystal violet staining of cells and determination of growth kinetics were performed as described previously (11). For growth kinetics, cell culture supernatants from the first cell culture passage after transfection were used.

RNA preparation, Northern (RNA) hybridization, RT-PCR, molecular cloning, and nucleotide sequencing. Methods for RNA preparation, Northern (RNA) hybridization, RT-PCR, molecular cloning, and nucleotide sequencing were described previously (10, 27). The following primer pairs were used for RT-PCR analyses as described in Results: primer pair 1 consisted of Ol Alfort-170 (5′-GTACAGGACAGTCGTCAGTAG-3′ [nt 171 to 191])/Ol Alfort-1423R (5′-AGTTACACCATCCATGTTTGTTCCATTCATG-3′ [nt 1393 to 1423]), primer pair 2 consisted of Ol Alfort-411 (5′-CAAACAAAAACCAGTGGGAG TG-3′ [nt 411 to 432])/Ol Alfort-994R (5′-TTGCATCAGGAGGCTTGGTC-3′ [nt 975 to 994]), and primer pair 3 consisted of Ol Alfort-170/Ol CSFV5.2 (5′-AACTCCATGTGCCATGTACAG-3′ [nt 360 to 380]).

Quantitative real-time RT-PCR. For comparative quantification of viral genomic RNAs, SK-6 cells were infected with supernatants from the second passage of CSFV strains Alfort-Jiv and Alfort-p447 at a multiplicity of infection (MOI) of 0.5; mock-infected SK-6 cells served as a negative control. Total cellular RNA was prepared 24 h p.i. Subsequently, photometric analyses were performed to determine the RNA concentration for each sample. Five microliters of each sample (containing 1.0 to 1.4 μg RNA/μl) was subjected to real-time RT-PCR analysis. For comparative quantification of viral genomic RNAs present in leukocyte preparations, about 1 μg of RNA obtained from leukocyte samples was used. After RT using the reverse pestivirus-specific primer pv03R (5′-TCCATGTGCCATGTACAGCAG-3′), the 28S RNA-specific reverse primer 28s02R (5′-GGGTCGGGAGTGGGTAATTT-3′), and Superscript II reverse transcriptase (Invitrogen, Karlsruhe, Germany), the quantitative real-time PCR was run using the AbiPrism7000 sequence detection system (Applied Biosystems, Branchburg, NJ) in the "Absolute Quantification" mode and Absolute QPCR Sybr green Rox mix (ABgene Ltd., Hamburg, Germany). For PCR amplification of CSFV-specific RNA, primer pair pv02 (5′-GTGGACGAGGGCA TGCC-3′ [sense primer])/pv03R was used. Cycling conditions were 1 cycle (2 min at 50°C and 10 min at 95°C) followed by 40 cycles (15 s at 95°C and 1 min at 60°C). For comparative quantification of cellular 28S RNA, primer pair 28s02R/28s01 (5′-CG GAGAGGGAGCCTGAGAA-3′ [sense primer]) was used in a separate reaction under the conditions described above. To compare the amounts of viral genomic RNA that accumulated in cells infected with CSFV Alfort-Jiv to that of parent strain Alfort-p447, we used the formula % RNA = $1/(2^{\Delta CT}) \times 100$. Finally, the results obtained were relativized according to the different amounts of 28S RNA.

Indirect IF and immunoblot analysis. Infection with CSFV was detected by indirect IF with monoclonal antibody (MAb) A18 directed against glycoprotein E2 (78). Immunoblot analyses were performed essentially as previously described (27). For the detection of NS3 and NS2-3, MAb 8.12.7 (21), kindly provided by E. J. Dubovi (Cornell University, Ithaca, NY), was used. The anti-MxA MAb M143 (24) was generously provided by O. Haller and G. Kochs (University of Freiburg, Freiburg, Germany). The antiserum against porcine interferon (IFN) regulatory factor 3 (IRF3) was kindly provided by N. Ruggli (Institute of Virology and Immunoprophylaxis, Mittelhäusern, Switzerland) (8). For infections of SK-6 cells (detection of NS3 and NS2-3) and PK-15 cells (detection of IRF3 and MxA), cell culture supernatants from the first and second cell culture passage after transfection were used, respectively.

Experimental design of the animal study. The animal experiment was performed at the high-containment unit of the Institute of Virology, University of Veterinary Medicine, Hannover, Germany. Fifteen piglets aged about 6 weeks were purchased from a commercial pig breeder, tested for the absence of neutralizing antibodies against pestiviruses, and randomly allocated to three groups of five animals each. All piglets were housed in one building, with each group in a separate compartment. After 1 week of acclimatization under standard high-security conditions of the European Community Reference Laboratory for CSF, the animals were infected with either cp CSFV Alfort-Jiv (group 1, animals 36 to 40) or non-cp CSFV Alfort-p447 (group 2, animals 41 to 45) both intranasally and intramuscularly (1.0×10^6 50% tissue culture infective doses [$TCID_{50}$] per route). Five uninfected animals served as a control (group 3). All piglets were monitored daily for clinical reactions including pyrexia. The clinical parameters were scored as described elsewhere previously; the scores ranged between 0 points (no clinical signs) and 27 points (most severe clinical symptoms) (53). At days 0, 2, 4, 7, 10, 14, 21, and 28 p.i. as well as at the day of death, all animals were sampled for venous blood derived from the vena jugularis externa. EDTA blood samples (days 0, 2, 4, 7, 10, 14, 21, and 28 p.i.) and serum samples (days 0, 14, 21, and 28 p.i. and day of death) were used for the determination of leukocyte counts, viremia, RT-PCR analyses of leukocyte-derived RNA preparations, and virus neutralization assays. Animals 41 (day 21 p.i.), 42 (day 22 p.i.), and 45 (day 15 p.i.) were euthanized before the end of the animal experiment due to the manifestation of severe clinical disease. Animal 43, showing a chronic course of CSF, and animal 44, which recovered from disease, were euthanized by intravenous injection of pentobarbital (Narcoren; Merial, Halbergmoos, Germany) at days 43 and 44 p.i., respectively. All remaining animals were euthanized at day 29 p.i. After euthanasia, all animals were subjected to postmortem pathological examination according to the standard protocol of the European Community Reference Laboratory for CSF.

Leukocyte counts. Manual leukocyte counts were performed after erythrocyte lysis by 2% acetic acid using an improved Neubauer counting cell chamber.

Virus isolation from leukocytes. Leukocytes were prepared from EDTA blood samples by use of an EDTA-dextran solution according to the guidelines of the European Union diagnostic manual for CSF diagnosis and the technical annex accompanying it (1) and used for the inoculation of Rie 5-1 cells. Pestivirus-specific antigen was detected after one blind passage of the supernatant obtained from inoculated cells by a peroxidase-linked antibody assay (see below) according to the guidelines of the European Union diagnostic manual for CSF diagnosis (1) or by IF analysis (see above).

Virus neutralization assays. Virus neutralization assays were performed as a neutralization peroxidase-linked antibody assay according to the guidelines of the European Union diagnostic manual for CSF diagnosis and its technical annex (1). CSFV Alfort-p447 and Rie 5-1 cells were used as a virus strain and cell line, respectively. Indirect immunostaining was performed with pestivirus-specific MAb BVD/C16 and a peroxidase-labeled secondary antibody (Dako, Hamburg, Germany).

RESULTS

Generation of CSFV Alfort-Jiv. The major goals of the present study were (i) to generate a genetically stable HVI CSFV strain that is capable to induce a CPE in various cell cultures and (ii) to investigate whether the cytopathogenicity of such a CSFV strain correlates with changes in virulence. With regard to data from a previous study, large duplications of viral sequences in the 3′ terminal part of the viral genome resulted in the genomic instability of HVI cp CSFV strains upon 10 passages in tissue culture cells (27). Alternatively, we now designed a CSFV strain carrying the sequences responsible for viral cytopathogenicity in the 5′ terminal part of the viral genome. For the closely related BVDV, several cp strains that harbor genomic rearrangements together with insertions of cellular sequences in the 5′ terminal genomic region were described previously (55, 56). For cp BVDV strain CP8, a 1.539-kb insertion (C^*-$N^{pro}*$) is located between the N^{pro} and C genes, which encodes a 513-aa fusion peptide consisting of fragments from viral sequences (C^*, $E^{rns}*$, and $N^{pro}*$) and cellular sequences (JivI, JivII, and bovine homologue to human nuclear protein Hcc-1 [Hcc-1*]) (55). In the BVDV system, the C^*-$N^{pro}*$ fusion peptide induced efficient NS2-3 cleavage in *trans*, which correlated with the release of large amounts of NS3 and viral cytopathogenicity (55). Accordingly, for the design of a new type of HVI cp CSFV, the CP8-derived cDNA fragment encoding C^*-$N^{pro}*$ was precisely inserted between the N^{pro} and C genes of the infectious cDNA clone of non-cp CSFV Alfort-p447, resulting in the generation of CSFV Alfort-Jiv (Fig. 1).

Growth characteristics of CSFV Alfort-Jiv. To investigate whether CSFV Alfort-Jiv is infectious and able to induce a CPE in different cell lines, porcine SK-6 and bovine MDBK cells were transfected with about 3.0 μg of synthetic Alfort-Jiv RNA. As controls, aliquots of both cell lines were either transfected with in vitro-transcribed RNA of parental non-cp CSFV Alfort-p447 or mock transfected. Twenty-six hours posttransfection, a CPE was detectable only in cells transfected with Alfort-Jiv RNA (Fig. 2A and data not shown). Compared to

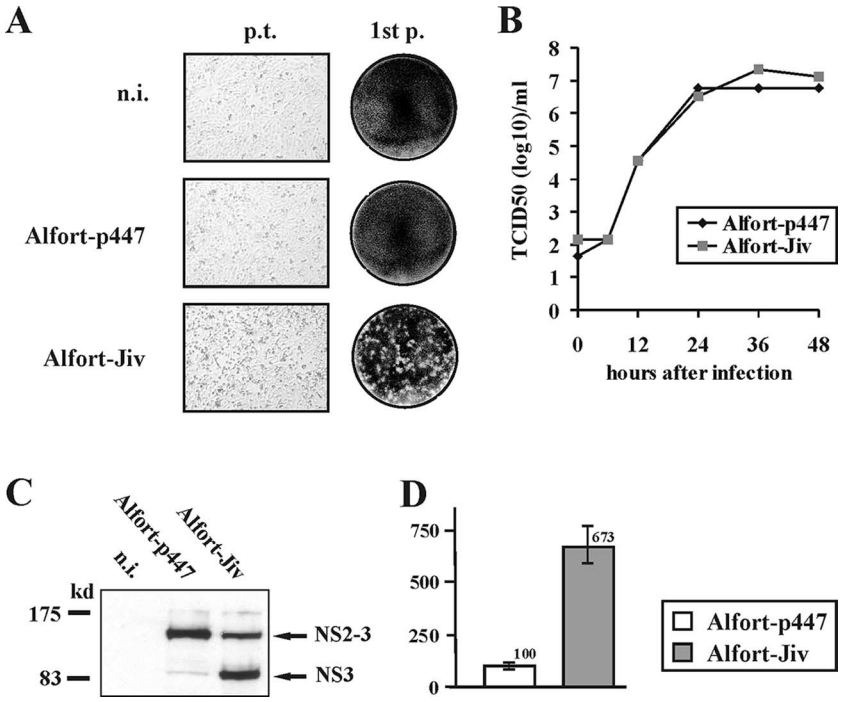

FIG. 2. Characterization of CSFV Alfort-Jiv in vitro. (A) Cytopathogenicity of Alfort-Jiv. (Left column) SK-6 cells were either mock transfected (top) or transfected with synthetic Alfort-p447 (middle) or Alfort-Jiv RNA (bottom). Twenty-six hours posttransfection, a CPE was detectable only in cells transfected with Alfort-Jiv RNA. (Right column) Cell culture supernatants from transfections were used to perform plaque assays. Six days p.i., plaques were visible only in cells infected with supernatant from cells transfected with Alfort-Jiv RNA. (B) Growth curves of cp CSFV Alfort-Jiv and non-cp CSFV Alfort-p447. Growth kinetics were determined on SK-6 cells infected at an MOI of 0.5. Titers of released virus were determined over a 2-day period at the indicated time points. (C) Immunoblot analysis of NS2-3 cleavage. SK-6 cells were infected with Alfort-p447 or Alfort-Jiv at an MOI of 1 and lysed 27 h p.i. The samples were subjected to sodium dodecyl sulfate-polyacrylamide gel electrophoresis under reducing conditions, transferred onto a nitrocellulose membrane, and analyzed by using anti-NS3 MAb 8.12.7. Marker proteins are indicated in kilodaltons on the left. The positions of NS2-3 and NS3 are indicated on the right. Note the large amount of NS3 detected from cells infected with Alfort-Jiv. n.i., noninfected SK-6 cells. (D) Relative amounts of accumulated viral genomic RNAs obtained 24 h after infection of SK-6 cells with CSFV Alfort-p447 and Alfort-Jiv at an MOI of 0.5. The graph shows mean values and standard deviations (error bars) obtained by quantitative real-time RT-PCR analysis, including the measurements of three independent replicates. The amount of CSFV RNA measured in cells infected with reference strain Alfort-p447 was set to 100%.

porcine SK-6 cells, the transfection of bovine MDBK cells with Alfort-Jiv RNA resulted in a less severe CPE (data not shown). These observations confirm previously reported findings that bovine cells are less susceptible to infections with CSFV than porcine cells (63) and show reduced plaque sizes after infection with cp CSFV (27). Furthermore, cell culture supernatants obtained from transfected SK-6 cells were used for infections of SK-6 cells and subsequent cell culture passages. Again, only cells infected with Alfort-Jiv showed a CPE characterized by cell lysis and the formation of plaques (Fig. 2A). Moreover, a similar CPE was also detected after infection of porcine Rie 5-1 and PK-15 cells with Alfort-Jiv (data not shown). In contrast, infections of SK-6, Rie 5-1, and PK-15 cells with non-cp CSFV Alfort-p447 did not result in a CPE (Fig. 2A and data not shown).

To evaluate the growth kinetics of Alfort-Jiv in comparison to parental Alfort-p447, growth rates and virus yields were determined using SK-6 cells infected at an MOI of 0.5. Virus released into the medium was sampled over a 2-day period, and the respective virus titers were determined by light microscopy (Alfort-Jiv) and IF analyses (Alfort-p447 and Alfort-Jiv). For Alfort-Jiv, infectious virus titers determined by light microscopy and IF analysis were identical. The peak titer of Alfort-Jiv reached at 36 h p.i. was 2.2×10^7 $TCID_{50}$/ml (Fig. 2B). At 48 h p.i., the titer decreased slightly, probably due to progressing cell lysis. For the parental non-cp CSFV strain Alfort-p447, the peak titer of 5.8×10^6 $TCID_{50}$/ml was reached at 24 h p.i. and did not significantly change until 48 h p.i. Similar results were obtained by two additional comparative analyses of the growth kinetics of Alfort-p447 and Alfort-Jiv (data not shown). Taken together, our analyses demonstrated that Alfort-Jiv is able to efficiently replicate in SK-6 cells and to induce a CPE on different porcine and bovine cell lines.

NS2-3 processing of CSFV Alfort-Jiv. The cytopathogenicity of pestiviruses including CSFV has been demonstrated to correlate with the expression of large amounts of NS3, the C-terminal part of NS2-3 (4, 9, 12, 27, 50, 51, 57, 71). Therefore, free NS3 is a hallmark of cp pestiviruses. However, compared to non-cp BVDV, where NS3 is usually no more detectable after the first 12 h p.i. (39), for non-cp BDV and non-cp CSFV strains, small amounts of NS3 can also be detected at later phases of infection (14, 51). To study the expression of uncleaved NS2-3 and free NS3 in cells infected with cp CSFV Alfort-Jiv, an immunoblot analysis was performed. The results of this analysis demonstrated that in cells infected with Alfort-Jiv, NS2-3 was efficiently processed, resulting in the expression

of large amounts of NS3 (Fig. 2C). In contrast, large amounts of NS2-3 but only very small amounts of NS3 were detected in cells infected with parental non-cp CSFV Alfort-p447. Taken together, the cytopathogenicity of CSFV Alfort-Jiv correlates with the expression of large amounts of NS3, an essential component of the viral replicase.

Quantification of viral RNA. For the related BVDV, it was previously reported that cp viruses produce larger amounts of viral genomic RNA than non-cp viruses (13, 46, 76). To investigate whether similar differences between cp CSFV Alfort-Jiv and non-cp Alfort-p447 exist, a CSFV-specific real-time RT-PCR analysis was performed. For comparative quantification of viral genomic RNAs, SK-6 cells were infected with cp CSFV Alfort-Jiv and non-cp CSFV Alfort-p447 at an MOI of 0.5; infections were performed in parallel with infections of cells used for the determination of growth kinetics (see above). Total cellular RNAs were prepared at 24 h p.i. and subjected to quantitative real-time RT-PCR; at this time point, the titers of infectious virus were similar for both viruses (Fig. 2B). Two independent quantitative real-time RT-PCR analyses, each including the measurement of three independent replicates for each of the samples, revealed that after the infection of cells with cp Alfort-Jiv, the amount of accumulated viral RNA was about seven times higher than the amount obtained from non-cp Alfort-p447-infected cells (Fig. 2D and data not shown).

Genetic stability of CSFV Alfort-Jiv during cell culture passages. cp BVDV and CSFV genomes carrying duplications of viral sequences can undergo genetic changes including various genomic deletions. According to previously reported studies, a limited number of cell culture passages of such cp pestiviruses may result in the emergence of non-cp viruses or viral subgenomes (6, 13, 26, 27). To examine the genetic stability of cp CSFV Alfort-Jiv during cell culture passages, a virus stock was generated using cell culture supernatant harvested 2 days after transfection with Alfort-Jiv RNA (first passage). This stock was then used for the additional nine subsequent SK-6 cell culture passages that were performed every 2 days by infecting 1.0×10^7 naive SK-6 cells with 2 ml of supernatant derived from the previous passage. The possible emergence of non-cp CSFV during cell culture propagation of Alfort-Jiv was monitored by IF analyses of virus titrations performed with supernatants of the 2nd and 10th passages. The respective IF analyses did not provide any evidence for the emergence of non-cp virus (data not shown).

In addition, the genetic stability or instability of Alfort-Jiv was investigated by Northern blot and RT-PCR analyses by using total cellular RNAs derived from transfected and infected (2nd and 10th passages) SK-6 cells. Total cellular RNAs from cells infected with Alfort-p447 and from noninfected cells as well as synthetic Alfort-p447 and Alfort-Jiv transcripts served as controls. Northern blot analysis indicated that upon cell culture passages of Alfort-Jiv, the size of the Alfort-Jiv genome was maintained, and genomic deletions were not detectable (Fig. 3A).

Moreover, RT-PCR analyses using oligonucleotides Alfort-170 and Alfort-1423R (Fig. 1) resulted in the amplification of a specific product of about 1.25 kb only when synthetic Alfort-p447 RNA or total cellular RNAs from cells either transfected with Alfort-p447 RNA or infected with Alfort-p447 were used

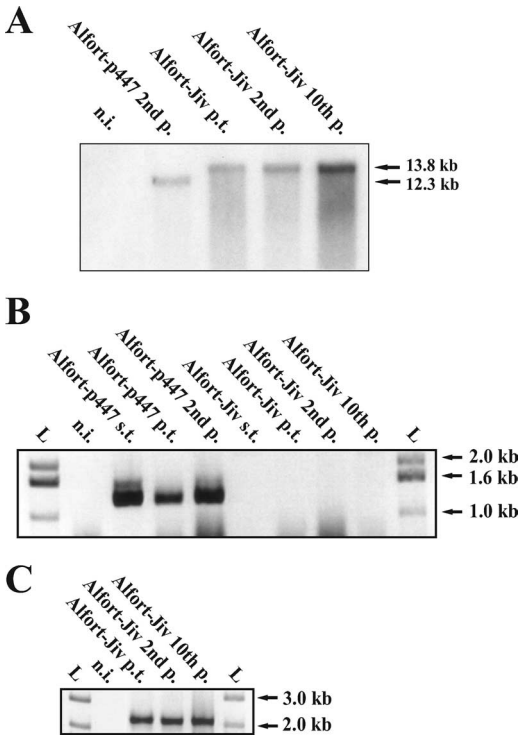

FIG. 3. Analysis of genetic stability of Alfort-Jiv. (A) Northern blot analysis of total cellular RNAs from SK-6 cells after infection with CSFV Alfort-p447 (second cell culture passage [p.]) and Alfort-Jiv (2nd and 10th passages) or after transfection with cp CSFV Alfort-Jiv RNA. For hybridization, a radioactively labeled EcoRI/NaeI cDNA fragment of pAlfort-p447 (2.8 kb) was used (27). Migration positions and sizes of the viral RNA genomes of Alfort-p447 and Alfort-Jiv are indicated in kilobases on the right. RNA from noninfected cells (n.i.) served as a negative control. Note that in the samples derived from passages of Alfort-Jiv, no additional bands corresponding to the emergence of non-cp CSFV or viral subgenomes are present. (B) RT-PCR analysis of synthetic genomic transcripts (s.t.) from CSFV Alfort-p447 and CSFV Alfort-Jiv, of total cellular RNAs from SK-6 cells harvested 26 h posttransfection (p.t.) with CSFV Alfort-p447 or CSFV Alfort-Jiv RNA, and of RNAs from cells infected with Alfort-p447 (second cell culture passage) or Alfort-Jiv (2nd and 10th cell culture passages). RNA from noninfected cells (n.i.) served as a negative control. The lengths of a size standard (L) are depicted in kilobases on the right. For RT-PCR, oligonucleotides Alfort-170 and Alfort-1423R (Fig. 1) were used. Note that specific RT-PCR products of about 1.25 kb (indicating the absence of the C*-N^{pro}* insertion) were obtained only for samples derived from Alfort-p447. (C) RT-PCR analysis of synthetic genomic transcripts from CSFV Alfort-Jiv, of total cellular RNA from SK-6 cells harvested 26 h posttransfection with Alfort-Jiv RNA, and of RNAs from cells infected with Alfort-Jiv (2nd and 10th passages). For RT-PCR, oligonucleotides Alfort-411 and Alfort-994R (Fig. 1) were used. Note that specific RT-PCR products of about 2.1 kb (indicating the presence of the complete C*-N^{pro}* insertion) were obtained for all samples derived from infections with Alfort-Jiv.

(Fig. 3B). In contrast, specific products of the same or similar size were not obtained when synthetic Alfort-Jiv RNA or RNAs from cells transfected with Alfort-Jiv RNA or infected with Alfort-Jiv (2nd and 10th cell culture passages) were investigated (Fig. 3B). Again, these analyses showed the absence of genomic deletions (eliminating most of or the entire C*-N^{pro}* coding sequence) for the Alfort-Jiv-derived samples. In addition, RT-PCR analyses using oligonucleotides Alfort-411

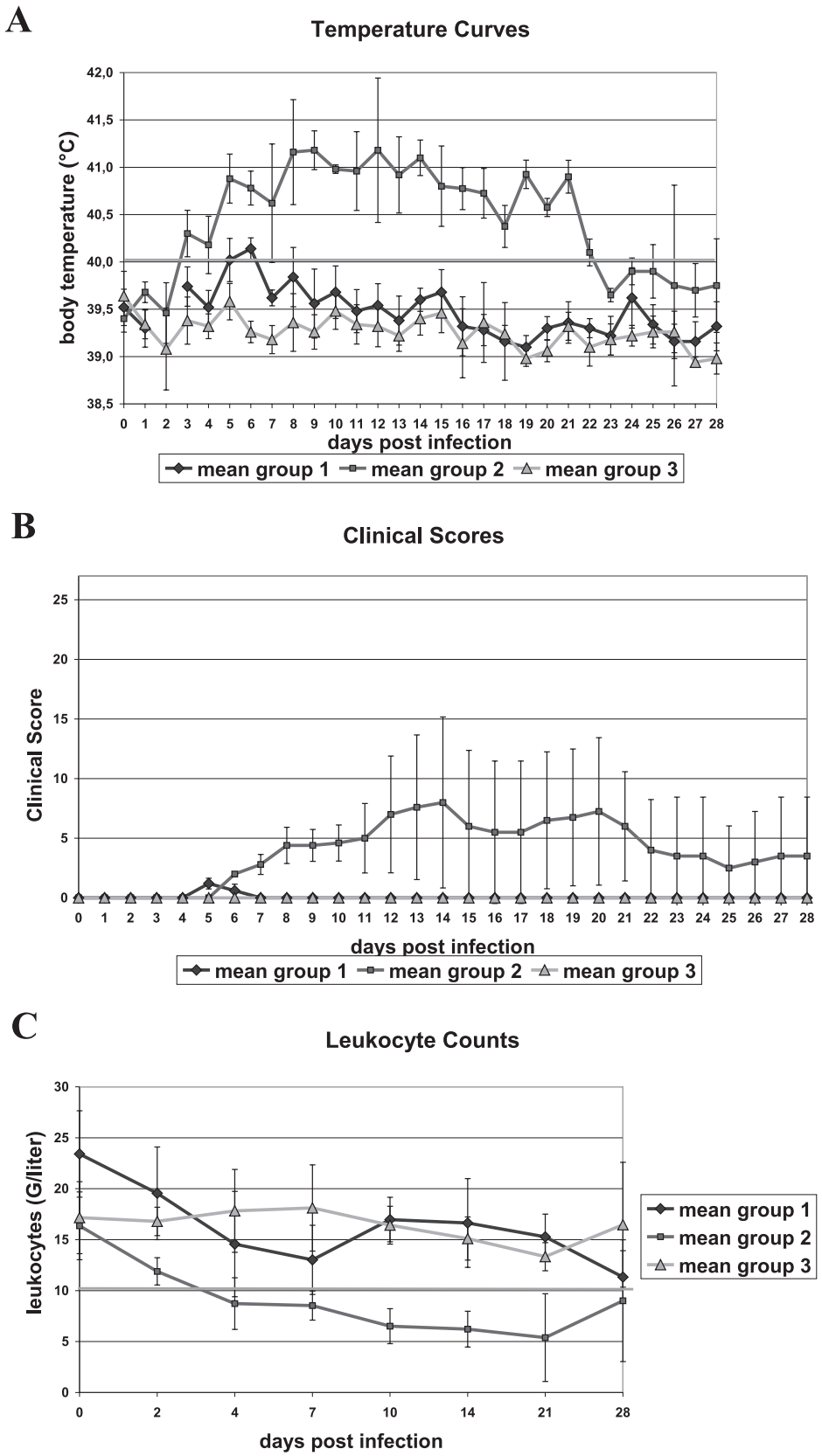

FIG. 4. Virulence of cp CSFV. (A) Mean body temperature curves of animals infected with cp CSFV Alfort-Jiv (group 1) or with non-cp Alfort-p447 (group 2). Each group consisted of five piglets that were infected both intranasally and intramuscularly with 1.0×10^6 $TCID_{50}$. Five mock-infected animals (group 3) served as a control. Temperatures were measured daily at the indicated time points. Temperatures

and Alfort-994R demonstrated a specific product of about 2.1 kb (indicating the presence of the complete C*-N^{pro}* insert) (Fig. 1) only for RNA samples obtained from cells transfected with synthetic Alfort-Jiv RNA or infected with Alfort-Jiv (2nd and 10th passages) (Fig. 3C). Finally, the specific RT-PCR product obtained from RNA of the 10th passage of Alfort-Jiv was cloned into a bacterial vector and subjected to nucleotide sequence analysis. This demonstrated the presence of the complete and unaltered C*-N^{pro}* insertion together with flanking viral sequences. Taken together, the results of the Northern blot and RT-PCR analyses showed that cp CSFV Alfort-Jiv was genetically stable during 10 cell culture passages.

Determination of virulence of CSFV Alfort-Jiv in piglets. Alfort-Jiv represents the first HVI CSFV strain that combines the ability to induce a CPE on different porcine cell lines with genetic stability during cell culture passages. Accordingly, Alfort-Jiv is suited to investigate whether the cytopathogenicity of CSFV correlates with changes of virulence in the natural host. To address this question, two groups of five piglets each were infected either with cp CSFV Alfort-Jiv (group 1, animals 36 to 40) or with the parental non-cp CSFV strain Alfort-p447 (group 2, animals 41 to 45). Five uninfected animals served as a control (group 3, animals 46 to 50). For the infection of animals, doses of 1.0×10^6 $TCID_{50}$ were applied both intranasally and intramuscularly.

In the course of infection, animals infected with non-cp Alfort-p447 (group 2) developed fever from day 2 or day 3 p.i. on. Animals 41, 42, and 45 remained febrile until euthanasia at days 21, 22, and 15 p.i., respectively. Animal 43 was febrile until day 29 p.i. but showed no fever at days 7, 23, and 27 p.i. Animal 44 was febrile until day 22 p.i. In contrast, animals infected with cp Alfort-Jiv (group 1) showed slightly increased body temperatures only at days 5 and/or 6 p.i. At later time points, only animals 38 (at day 24 p.i.), 39 (at day 8 p.i.), and 40 (at days 9 and 10 p.i.) sporadically showed slightly increased body temperatures (data not shown). With regard to the five control animals (group 3), only one animal showed a slight fever at the day of inoculation. Comparison of the mean values for each group demonstrated that infection with cp Alfort-Jiv resulted in slightly increased body temperatures only at days 5 and 6 p.i., while animals infected with parental non-cp Alfort-p447 developed significantly higher fever over a considerably longer period between days 3 and 22 p.i. (Fig. 4A).

Including the measurement of body temperatures, clinical symptoms were determined daily and evaluated within a range of 0 points (no clinical signs) and 27 points (most severe clinical symptoms) as described elsewhere previously (53). All animals infected with non-cp Alfort-p447 (group 2) showed typical symptoms of CSF such as general depression, anorexia, conjunctivitis, obstipation, diarrhea, respiratory symptoms, ataxia, and hemorrhages to variable extents. Due to the occurrence of severe disease, animals 41 (day 21 p.i.), 42 (day 22 p.i.), and 45 (day 15 p.i.) were euthanized before the end of the experiment. Animal 43 showed a chronic course of CSF, while animal 44 showed only mild disease symptoms and recovered until the end of the experiment. In contrast, animals infected with cp Alfort-Jiv and animals from the control group did not develop disease. When comparing the mean clinical scores for each group, only group 2 displayed significant clinical scores ranging between 3.0 and 7.2 from day 7 p.i. on (Fig. 4B).

After euthanasia, all animals were subjected to postmortem pathological examination. Animals 41, 42, 43, and 45 (group 2) showed significant pathomorphological signs of CSF to different extents, including hemorrhages in the skin, mucosa, tonsils, larynx, heart, and kidneys as well as cyanotic skin alterations; highly enlarged, edematous, and hemorrhagic lymph nodes; thymus atrophy; pneumonia; and catarrhal enteritis (data not shown). In contrast, animal 44, which recovered from disease, as well as all animals from group 1 (infected with Alfort-Jiv) and group 3 (uninfected) showed no changes typical for CSF.

It is known that infections with pestiviruses can induce leukopenia, thereby contributing to severity of disease. All animals infected with non-cp Alfort-p447 showed leukopenia to different extents. With respect to the mean values of group 2, leukocyte counts were below 10 G/liter (indicating leukopenia) from day 4 p.i. until the end of the experiment (Fig. 4C). In contrast, animals infected with cp Alfort-Jiv showed only slightly dropping leukocyte counts until day 7 p.i., after which the group's mean leukocyte count started to rise again; however, at no time did the mean value drop below 10 G/liter (Fig. 4C). Animals of control group 3 did not show leukopenia at any time.

To measure the extent and duration of cell-bound viremia and viral genome load, virus isolations and RT-PCR analyses were performed. For virus isolation, leukocytes were prepared from EDTA blood samples (group 1 at days 0, 4, 7, 10, and 14 p.i. and group 2 at days 7 and 10 p.i.) and used for the inoculation of porcine kidney Rie 5-1 cells. CSFV antigen was detected after one blind passage of the supernatant obtained from inoculated cells by a peroxidase-linked antibody assay. CSFV was isolated from all samples derived from animals infected with Alfort-p447. With respect to the animals infected with Alfort-Jiv, CSFV was detected only from one single sample obtained from animal 38 at day 7 p.i. (data not shown). In contrast, for all other samples derived from animals of group 2, CSFV could not be isolated. Moreover, the presence of CSFV genomic RNA in leukocyte preparations of infected animals was investigated by RT-PCR analyses. For all piglets infected with cp Alfort-Jiv, CSFV RNA was detectable only in samples derived from day 7 p.i. (Table 1). In contrast, samples of animals infected with Alfort-p447 were positive for CSFV

higher than 40°C (threshold line) were considered to be febrile. Bars indicate standard deviations. (B) Mean clinical scores of groups 1 to 3. Clinical symptoms including body temperatures were monitored daily and evaluated within a range of 0 points (no clinical signs) and 27 points (most severe clinical symptoms) as described elsewhere previously (53). Note that only animals of group 2 showed clinical signs of disease from day 7 p.i. on. Bars indicate standard deviations. (C) Mean leukocyte counts of blood samples obtained from animals of groups 1 to 3. Samples were taken over 4 weeks at the indicated time points. Leukocyte counts below 10 G/liter (threshold line) were considered leukopenia. Note that only mean values of group 2 demonstrated leukopenia from day 4 on. Bars indicate standard deviations.

TABLE 1. RT-PCR analyses of leukocyte preparations for detection of CSFV RNA[a]

Animal	Detection of CSFV RNA at day p.i.:					
	2	4	7	10	14	21
Group 1						
36	−	−	+	−	−	−
37	−	−	+	−	−	−
38	−	−	+	−	−	−
39	−	−	+	−	−	−
40	−	−	+	−	−	−
Group 2						
41	−	+	+	+	ND	+
42	−	+	+	+	+	+
43	−	+	+	+	+	+
44	+	+	+	+	+	−
45	−	+	+	+	+	E
Group 3 (pool)	−	−	−	−	−	−

[a] ND, not done; E, euthanized 15 days p.i.

RNA at days 4, 7, 10, 14, and 21 p.i. In addition, for animal 44, CSFV RNA was detected in samples collected at day 2 p.i. but not at day 21 p.i. Pooled samples of control group 3 were negative by RT-PCR analyses for all time points investigated. Moreover, for the samples derived from day 7 p.i., two independent quantitative real-time RT-PCR analyses each including the measurement of three independent replicates for each of the samples were performed. The results obtained showed that after infection of animals with Alfort-p447, the amounts of viral RNA were about 5 to 50 times higher than the amounts of viral RNA present in samples from animals infected with Alfort-Jiv (Fig. 5).

Taken together, the analyses of clinical scores including body temperatures, postmortem examination, leukocyte counts, the reduced duration of both CSFV viremia and genome load in leukocytes, and the significantly smaller amounts of viral RNA present in leukocytes at day 7 p.i. demonstrate that cp CSFV Alfort-Jiv is highly attenuated in the natural host compared to the parental non-cp CSFV strain Alfort-p447.

Induction of neutralizing antibodies. To determine whether and to what extent infections with Alfort-p447 and Alfort-Jiv led to the induction of CSFV-neutralizing antibodies, virus neutralization assays were performed. For all animals infected with Alfort-Jiv, moderate to high levels of CSFV-neutralizing antibodies that reached reciprocal serum titers of more than 300 50% neutralizing doses at day 21 p.i. were induced (Fig. 6A); similar titers of neutralizing antibodies are induced after natural infection of pigs with low-virulent CSFV field strains and after vaccination with currently used vaccines. In contrast, for piglets infected with Alfort-p447, only animal 44, which recovered from infection, reached similar titers of neutralizing antibodies, while for the remaining animals that showed an acute lethal or chronic courses of CSF, either no or only low titers of neutralizing antibodies were detected (Fig. 6B).

Viral growth of cp and non-cp CSFV in porcine PK-15 cells and effects on expression of IRF3 and the Mx protein. Our animal study revealed that in contrast to parental non-cp CSFV Alfort-p447, cp CSFV Alfort-Jiv is highly attenuated in pigs. It was therefore interesting to examine whether cp CSFV differs from non-cp CSFV with respect to the known interference with cellular antiviral defense mechanisms by non-cp pestiviruses (7, 8, 19, 33, 40, 64, 65, 68, 69). For these experiments, porcine type 1 IFN-competent PK-15 cells were used, as it was previously reported that SK-6 cells cannot be stimulated to produce type 1 IFN (65). Comparative analysis of viral replication in PK-15 cells revealed that the viral growth kinetics of Alfort-Jiv and Alfort-p447 were almost identical (Fig. 7A). Compared to viral replication in SK-6 cells (Fig. 2B), the peak titers of Alfort-p447 and Alfort-Jiv produced in PK-15 cells were about 15 and 50 times lower, respectively. Furthermore, in PK-15 cell cultures treated with 1.1 nanogram of recombinant human IFN-α2a per milliliter (added 1 h prior to infection), the titers obtained 24 h and 48 h after infection with cp Alfort-Jiv were about 100- to 200-fold lower than those for parallel infections of untreated PK-15 cells (Fig. 7B). A similar but slightly lower reduction of virus titers (about 20- to 50-fold) was also observed after infection of IFN-treated PK-15 cells with non-cp Alfort-p447. The addition of IFN at 14 h prior to infection with cp and non-cp CSFV led to very similar results (data not shown).

It has been established that pestiviruses counteract the antiviral type 1 IFN system by targeting IRF3 for proteasome-dependent degradation; the loss of IRF3 in infected cells is due to the action of the pestiviral N-terminal autoprotease N^{pro} (8, 33, 40, 64). One of the best-characterized antiviral proteins induced by type 1 IFNs is the Mx protein (31). To investigate the effects of cp and non-cp CSFV on the expression of IRF3 and the induction of Mx in PK-15 cells, cell lysates were prepared at 24 h and 48 h p.i., and aliquots of 2×10^4 and 2×10^5 cells were subjected to immunoblot analysis using an anti-IRF3 antiserum and an anti-Mx MAb, respectively. Infection with cp and non-cp CSFV resulted in the complete loss of IRF3 at 48 h p.i., while small amounts of IRF3 were detectable at 24 h p.i. (Fig. 7C). Interestingly, infection with cp Alfort-Jiv caused the induction of Mx expression despite the degradation of IRF3 (Fig. 7D). In contrast, Mx was not induced by non-cp Alfort-p447. Taken together, these findings indicate that the attenu-

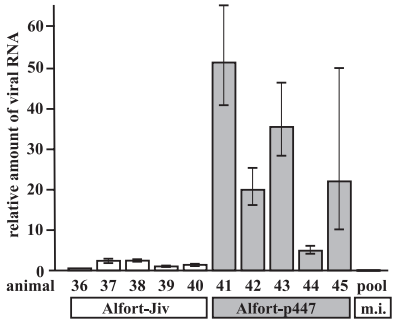

FIG. 5. Relative amounts of viral genomic RNAs present in leukocyte preparations obtained from animals at 7 days after infection with CSFV Alfort-Jiv (animals 36 to 40) (white bars) and Alfort-p447 (animals 41 to 45) (gray bars) and from pooled samples of the mock-infected animals (pool). The graph shows mean values and standard deviations (error bars) obtained by quantitative real-time RT-PCR analysis including the measurements of three independent replicates. The amount of CSFV RNA measured in the sample from animal 39 was set to 1.

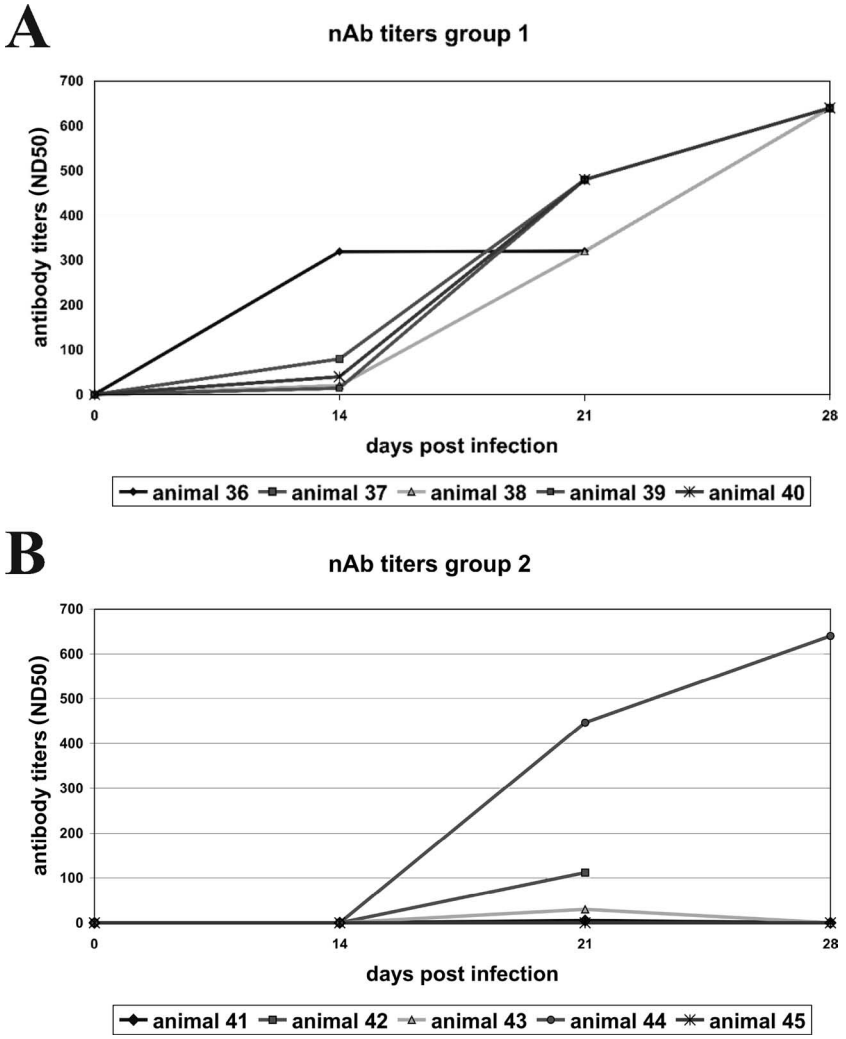

FIG. 6. Induction of neutralizing antibodies against CSFV. Neutralizing antibody (nAb) titers are given for serum samples derived from animals infected with cp CSFV Alfort-Jiv (group 1, animals 36 to 40) (A) or non-cp Alfort-p447 (group 2, animals 41 to 45) (B). Blood samples were taken at the indicated time points, and reciprocal neutralizing antibody titers were determined by a neutralization peroxidase-linked antibody assay as 50% neutralizing doses (ND50) using Alfort-p447 as the test virus. Animals 41 (day 21 p.i.), 42 (day 22 p.i.), and 45 (day 15 p.i.) were euthanized before the end of the animal experiment due to the occurrence of severe clinical symptoms. Note that high titers of neutralizing antibodies were induced after infection with cp CSFV Alfort-Jiv (all animals of group 1), whereas for animals infected with parental non-cp CSFV Alfort-p447 (group 2), only animal 44 developed significant titers.

ation of cp Alfort-Jiv in the animal correlates with the induction of cellular antiviral defense.

DISCUSSION

A remarkable feature of all established pestivirus species including BVDV and CSFV is the existence of cp and non-cp viruses. A number of studies concentrated on the characterization of genomes and biological properties of various cp BVDV strains, while our knowledge about the cytopathogenicity of CSFV is limited. In particular, it is not known so far whether cp CSFV differs from non-cp CSFV with respect to virulence. In this study, we have generated Alfort-Jiv, a novel type of cp CSFV, by introducing a Jiv90-containing fragment into the genome of moderately virulent non-cp CSFV strain Alfort-p447. Our analyses demonstrated that (i) the protein encompassing Jiv90 is able to induce the cleavage of NS2-3 of CSFV in *trans*, (ii) the cytopathogenicity of CSFV Alfort-Jiv correlates with enhanced viral RNA replication, (iii) cp CSFV Alfort-Jiv is strongly attenuated in its natural host, and (iv) the attenuation of cp CSFV correlates with its inability to block the induction of the antiviral Mx protein.

In contrast to cp BVDV, all known cp CSFV field isolates represent helper virus-dependent subgenomes that lack the genomic region encoding the structural proteins as well as N^{pro}, p7, and NS2 (2, 3, 36, 51). Accordingly, all previous studies that investigated biological differences between cp and non-cp CSFV isolates compared the properties of non-cp CSFV in the presence and absence of such cp CSFV subgenomes. Recently, we reported the generation of the first helper virus-independent cp CSFV strain CP G1 that is capable of inducing a CPE on various porcine and bovine cell lines (27).

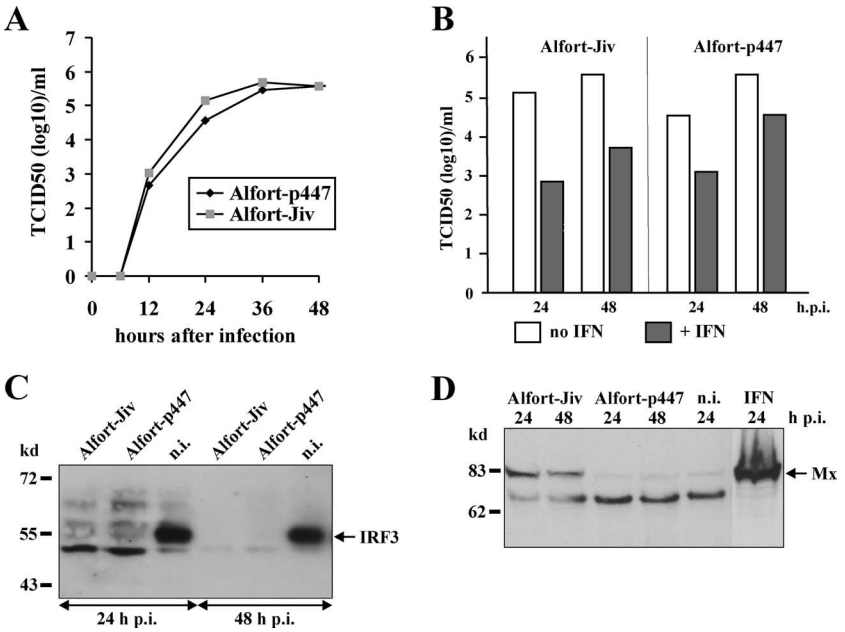

FIG. 7. Viral growth of Alfort-Jiv and Alfort-p447 in porcine PK-15 cells and effects on expression of IRF3 and the Mx protein. (A) Growth curves of cp CSFV Alfort-Jiv and non-cp CSFV Alfort-p447. Growth kinetics were determined on PK-15 cells infected at an MOI of 0.5. Titers of released virus were determined over a 2-day period at the indicated time points. (B) Virus titers obtained 24 h and 48 h after infection of untreated PK-15 cells (white bars) and PK-15 cell cultures treated with 1.1 nanogram of recombinant human IFN-α2a per milliliter at the time of infection (gray bars). Infections with cp Alfort-Jiv and non-cp Alfort-p447 were performed at an MOI of 0.5. (C and D) Expression of IRF3 (C) and Mx (D). Porcine PK-15 cells were infected with cp Alfort-Jiv and non-cp Alfort-p447 at an MOI of 1 and incubated for 24 h or 48 h at 37°C; noninfected (n.i.) cells served as a negative control. Cells were lysed at the time points indicated and subjected to immunoblot analysis. The samples (each containing the material from about 2×10^4 cells) were separated by sodium dodecyl sulfate-polyacrylamide gel electrophoresis under reducing conditions, transferred onto nitrocellulose, and incubated with an antiserum against porcine IRF3 (C). For the detection of Mx, the samples each contained material from about 2×10^5 cells, and anti-human Mx MAb M143 was used (D). Ten nanograms of recombinant human IFN-α2a per milliliter was used as a positive control for the expression of the Mx protein. Due to the expression of very large amounts of the Mx protein after treatment of cells with IFN, an about 10-times-shorter exposure time of the autoradiograph is shown for this lane.

Unfortunately, this cp CSFV strain, whose genome contains duplicated viral sequences together with an insertion of ubiquitin-coding sequences, was shown to be genetically unstable, resulting in various kinds of deletions during a limited number of tissue culture passages. Therefore, this strain was not appropriate to study the virulence of cp CSFV in the natural host. In contrast, cp CSFV strain Alfort-Jiv described in this study combines helper virus-independent replication and genetic stability during propagation in tissue culture cells and thus is well suited to compare the properties of cp and non-cp CSFV in both susceptible cells and the natural host.

The cytopathogenicity of pestiviruses including BVDV, BDV, and CSFV has been shown to correlate with the expression of large amounts of NS3, the C-terminal part of NS2-3 (5, 9, 20, 21, 23, 27, 30, 51). The genetic background and the resulting molecular mechanisms that lead to the efficient release of free NS3 are remarkably diverse among cp pestivirus genomes, including (i) genomic deletions fusing the translation start codon (51) or the autoprotease N^{pro} gene (72) directly to the 5′ end of the viral NS3 gene, (ii) duplicated viral sequences located in the NS2 gene (70), (iii) point mutations in the NS2 gene (37), and (iv) the insertion of cleavage sites for cellular proteases directly upstream of NS3 (6, 12, 16, 25, 71). Representing yet another different prototype of cp pestiviruses, Alfort-Jiv contains Jiv-coding sequences, which are part of the cp BVDV CP8-derived insertion C^*-N^{pro*} (55). Apart from BVDV CP8 and CSFV Alfort-Jiv, the genomes of several other cp pestivirus strains contain Jiv-coding sequences that are either also located in the 5′-terminal genomic region (56) or inserted into the NS2 gene (see, for example, references 5, 9, and 46). Jiv is known to induce the cleavage of BVDV NS2-3 in *cis* (46) and in *trans* (59), a mechanism that is based on the activation of the NS2 autoprotease (38, 39). The results of our in vitro experiments with CSFV Alfort-Jiv show that Jiv also activates the NS2 autoprotease of CSFV in *trans* and thereby leads to the expression of large amounts of NS3 (Fig. 2C) and viral cytopathogenicity (Fig. 2A). The former observation is supported by recently published data. The expression of CSFV NS2-3-4A in the presence of cofactor Jiv90 was shown to result in the cleavage of NS2-3; this cleavage could be completely abolished by mutations of the catalytic histidine and cysteine residues within NS2 (54). Moreover, our study showed that after the infection of cells with cp Alfort-Jiv, the amount of accumulated viral RNA was significantly higher than that obtained from non-cp Alfort-p447-infected cells (Fig. 2D). Similar differences concerning the efficiency of viral RNA synthesis were reported previously for isogenic pairs of cp and non-cp BVDV (13, 46, 76). Taken together, NS2-3 cleavage and the resulting expression of large amounts of NS3, enhanced viral RNA replication, as well as viral cytopathogenicity are closely linked processes and represent common properties of cp Jiv-90 expressing pestiviruses including CSFV.

For BVDV, it is well known that the emergence of cp viruses in animals persistently infected with non-cp BVDV results in the induction of a severe and deadly disease, i.e., mucosal disease, while acute infections of naive nonpregnant animals with cp BVDV usually do not cause disease. For closely related CSFV, only helper virus-dependent cp field isolates have been reported. According to the literature, experimental infections of pigs with such combinations of cp subgenomes and non-cp helper viruses led to contradictory results, suggesting that the virulence of such combinations is either slightly increased (36) or attenuated (3) compared to that of the non-cp virus only. Therefore, it is not known so far whether HVI cp CSFV differs from non-cp viruses with respect to virulence. The results of our animal study show that in contrast to infection with moderately virulent non-cp CSFV Alfort-p447, infections with cp CSFV Alfort-Jiv did not cause disease including fever and leukopenia. Moreover, after infection of pigs with Alfort-Jiv, viremia was either not detectable or strongly restricted, and the duration of CSFV genomic load in leukocytes was significantly limited. Taken together, our results demonstrate that HVI cp CSFV is strongly attenuated in pigs.

Attenuation of viruses can result from various genetic changes that may lead to a general restriction of viral replication in susceptible cells or influence interactions between virus and host. It was previously reported that the virulence of non-cp CSFV can be significantly reduced by different kinds of mutations including, e.g., the deletion of the viral N^{pro} gene (45, 74), mutations abrogating the RNase activity of viral glycoprotein E^{rns} (48), mutations of N-glycosylation sites within the envelope proteins (62, 66), or the replacement of partial or entire E2 coding sequences by corresponding sequences from an avirulent CSFV vaccine strain (60, 61). The cp and non-cp CSFV strains compared in this study differ in a 1.539-kb insertion representing the genetic basis for cytopathogenicity of Alfort-Jiv in susceptible cells. As our in vitro studies clearly demonstrated that the insertion present in the genome of Alfort-Jiv had no negative effect on virus growth but rather increased the efficiency of viral replication and viral RNA synthesis (Fig. 2B and D and 7A), it appears very unlikely that the attenuation of cp CSFV Alfort-Jiv is the result of an intrinsic restriction of viral replication due to the large insertion of cp CSFV Alfort-Jiv in the genome. Alternatively, the attenuation of Alfort-Jiv including the observed strong reduction of viral replication in the animal might be due to differences in terms of antiviral defense.

The induction or suppression of antiviral defense mechanisms by pathogenic viruses significantly influences their ability to cause disease in the infected host (31). It is known that non-cp pestiviruses prevent the induction of type 1 IFN and thereby the expression of IFN-inducible antiviral proteins such as Mx (19, 64, 65, 68, 69). This property is mediated by the viral protein N^{pro}, which targets IRF3 for proteasome-dependent degradation (8, 33, 38, 64). In contrast to non-cp pestiviruses, cp BVDV and cp helper virus-dependent CSFV subgenomes are characterized by uncontrolled RNA genome replication and the inability to block an IFN response to double-stranded RNA (7, 39, 69). Our analysis demonstrated that infection of porcine PK-15 cells with helper virus-independent cp CSFV resulted in the induction of Mx expression, while infection with the parental non-cp CSFV did not (Fig. 7D). Accordingly, the attenuation of Alfort-Jiv is linked to its inability to block the induction of Mx, which is significantly implicated in host antiviral defense. Similar results have been reported for genetically engineered non-cp CSFV strains either lacking the N^{pro} gene or encompassing mutations abrogating the RNase activity of E^{rns}; these CSFV mutants are limited in their ability block the type 1 IFN system and are also attenuated in the natural host (45, 48, 74). In contrast to CSFV mutants lacking the N^{pro} gene, infection with cp Alfort-Jiv resulted in a complete loss of IRF3 (Fig. 7C). This suggests that the induction of Mx expression in cells infected with cp Alfort-Jiv may be independent of IRF3-dependent type 1 IFN induction. According to investigations of human and murine cells, it is believed that Mx is induced exclusively via signaling through the type 1 IFN receptor (77). However, a recent study provided evidence that in bovine cells, Mx can also be induced via a type 1 IFN signaling-independent pathway (68). Future studies will include analysis of IFN-β bioactivity in the supernatant of cp CSFV-infected cells in order to clarify whether the observed Mx expression is actually IFN-β independent. Furthermore, it will be interesting to study the effects of cp and non-cp CSFV on cellular antiviral defense in more detail, including investigations of primary target cells.

The ability of viruses such as non-cp CSFV to block the induction of IFN not only is important with respect to innate immune reactions against viral infections but also impacts the efficacy of adaptive immune responses, as type 1 IFNs are potent enhancers of immune responses (35, 42, 58). We show here for the first time that HVI cp CSFV induces the expression of Mx and that this stimulation of cellular antiviral defense observed in vitro correlates with strongly reduced viral replication and attenuation in the natural host. While it can be assumed that the reduced replication of cp Alfort-Jiv in the animal might result in a limited immunological response, the results of our study demonstrated that the amount of viral antigen produced after infection with Alfort-Jiv is apparently sufficient to elicit high titers of neutralizing antibodies. Taken together, HVI cp CSFV represents a promising candidate for the development of attenuated live virus vaccines against CSF with potent immunogenic properties.

ACKNOWLEDGMENTS

We thank S. Widauer, G. Müller, and G. Thiem for excellent technical assistance, M. König and S. Deike for helpful discussions, and H.-J. Thiel for support.

A.G. and S.G. were supported by SFB 535, Invasion Mechanisms and Replication Strategies of Infectious Agents, from the Deutsche Forschungsgemeinschaft (German Research Foundation).

REFERENCES

1. **Anonymous.** 2002. Commission decision of February 2002 approving a diagnostic manual establishing diagnostic procedures, sampling methods and criteria for evaluation of the laboratory tests for the confirmation of classical swine fever (2002/106/EC). Off. J. Eur. Union **L039:**78–88.
2. **Aoki, H., K. Ishikawa, Y. Sakoda, H. Sekiguchi, M. Kodama, S. Suzuki, and A. Fukusho.** 2001. Characterization of classical swine fever virus associated with defective interfering particles containing a cytopathogenic subgenomic RNA isolated from wild boar. J. Vet. Med. Sci. **63:**751–758.
3. **Aoki, H., K. Ishikawa, H. Sekiguchi, S. Suzuki, and A. Fukusho.** 2003. Pathogenicity and kinetics of virus propagation in swine infected with the cytopathogenic classical swine fever virus containing defective interfering particles. Arch. Virol. **148:**297–310.
4. **Aoki, H., Y. Sakoda, S. Nakamura, S. Suzuki, and A. Fukusho.** 2004. Cytopathogenicity of classical swine fever viruses that do not show the exaltation

of Newcastle disease virus is associated with accumulation of NS3 in serum-free cultured cell lines. J. Vet. Med. Sci. **66:**161–167.
5. **Avalos-Ramirez, R., M. Orlich, H.-J. Thiel, and P. Becher.** 2001. Evidence for the presence of two novel pestivirus species. Virology **286:**456–465.
6. **Baroth, M., M. Orlich, H.-J. Thiel, and P. Becher.** 2000. Insertion of cellular NEDD8 coding sequences in a pestivirus. Virology **278:**456–466.
7. **Bauhofer, O., A. Summerfield, K. C. McCullough, and N. Ruggli.** 2005. Role of double-stranded RNA and N^{pro} of classical swine fever virus in the activation of monocyte-derived dendritic cells. Virology **343:**93–105.
8. **Bauhofer, O., A. Summerfield, Y. Sakoda, J. D. Tratschin, M. A. Hofmann, and N. Ruggli.** 2007. Classical swine fever virus N^{pro} interacts with interferon regulatory factor 3 and induces its proteasomal degradation. J. Virol. **81:** 3087–3096.
9. **Becher, P., G. Meyers, A. D. Shannon, and H.-J. Thiel.** 1996. Cytopathogenicity of border disease virus is correlated with integration of cellular sequences into the viral genome. J. Virol. **70:**2992–2998.
10. **Becher, P., M. Orlich, M. König, and H.-J. Thiel.** 1999. Nonhomologous RNA recombination in bovine viral diarrhea virus: molecular characterization of a variety of subgenomic RNAs isolated during an outbreak of fatal mucosal disease. J. Virol. **73:**5646–5653.
11. **Becher, P., M. Orlich, and H.-J. Thiel.** 2000. Mutations in the 5′ nontranslated region of bovine viral diarrhea virus result in altered growth characteristics. J. Virol. **74:**7884–7894.
12. **Becher, P., M. Orlich, and H.-J. Thiel.** 1998. Ribosomal S27a-coding sequences upstream of ubiquitin-coding sequences in the genome of a pestivirus. J. Virol. **72:**8697–8704.
13. **Becher, P., M. Orlich, and H.-J. Thiel.** 2001. RNA recombination between persisting pestivirus and a vaccine strain: generation of cytopathogenic virus and induction of lethal disease. J. Virol. **75:**6256–6264.
14. **Becher, P., A. D. Shannon, N. Tautz, and H.-J. Thiel.** 1994. Molecular characterization of border disease virus, a pestivirus from sheep. Virology **198:**542–551.
15. **Becher, P., and H.-J. Thiel.** 2002. Genus *Pestivirus* (*Flaviviridae*), p. 327–331. *In* C. A. Tidona and G. Darai (ed.), The Springer index of viruses. Springer-Verlag, Heidelberg, Germany.
16. **Becher, P., H.-J. Thiel, M. Collins, J. Brownlie, and M. Orlich.** 2002. Cellular sequences in pestivirus genomes encoding gamma-aminobutyric acid (A) receptor-associated protein and Golgi-associated ATPase enhancer of 16 kilodaltons. J. Virol. **76:**13069–13076.
17. **Bolin, S. R., A. W. McClurkin, R. C. Cutlip, and M. F. Coria.** 1985. Severe clinical disease induced in cattle persistently infected with noncytopathogenic bovine viral diarrhea virus by superinfection with cytopathogenic bovine viral diarrhea virus. Am. J. Vet. Res. **46:**573–576.
18. **Brownlie, J., M. C. Clarke, and C. J. Howard.** 1984. Experimental production of fatal mucosal disease in cattle. Vet. Rec. **114:**535–536.
19. **Charleston, B., M. D. Fray, S. Baigent, B. V. Carr, and W. I. Morrison.** 2001. Establishment of persistent infection with non-cytopathic bovine viral diarrhoea virus in cattle is associated with a failure to induce type I interferon. J. Gen. Virol. **82:**1893–1897.
20. **Collett, M. S., R. Larson, S. Belzer, and E. Retzel.** 1988. Proteins encoded by bovine viral diarrhea virus: the genome organization of a pestivirus. Virology **165:**200–208.
21. **Corapi, W. V., R. O. Donis, and E. J. Dubovi.** 1988. Monoclonal antibody analyses of cytopathic and noncytopathic viruses from fatal bovine viral diarrhea infections. J. Virol. **62:**2823–2827.
22. **de Castro, M. P.** 1973. An infectious agent causing "spontaneous" degeneration of swine cells in vitro. In Vitro **9:**8–16.
23. **Donis, R. O., and E. J. Dubovi.** 1987. Characterization of bovine diarrhoea-mucosal disease virus-specific proteins in bovine cells. J. Gen. Virol. **68:** 1597–1605.
24. **Flohr, F., S. Schneider-Schaulies, O. Haller, and G. Kochs.** 1999. The central interactive region of human MxA GTPase is involved in GTPase activation and interaction with viral target structures. FEBS Lett. **463:**24–28.
25. **Fricke, J., C. Voss, M. Thumm, and G. Meyers.** 2004. Processing of a pestivirus protein by a cellular protease specific for light chain 3 of microtubule-associated proteins. J. Virol. **78:**5900–5912.
26. **Gallei, A., M. Orlich, H.-J. Thiel, and P. Becher.** 2005. Noncytopathogenic pestivirus strains generated by nonhomologous RNA recombination: alterations in the NS4A/NS4B coding region. J. Virol. **79:**14261–14270.
27. **Gallei, A., T. Rümenapf, H.-J. Thiel, and P. Becher.** 2005. Characterization of helper virus independent cytopathogenic classical swine fever virus generated by an in vivo RNA recombination system. J. Virol. **79:**2440–2448.
28. **Gillespie, J. H., J. A. Baker, and K. McEntee.** 1960. A cytopathogenic strain of virus diarrhea virus. Cornell Vet. **50:**73–79.
29. **Gillespie, J. H., B. E. Sheffy, and J. A. Baker.** 1960. Propagation of hog cholera virus in tissue culture. Proc. Soc. Exp. Biol. Med. **105:**679–681.
30. **Greiser-Wilke, I., K. E. Dittmar, B. Liess, and V. Moennig.** 1992. Heterogeneous expression of the non-structural protein p80/p125 in cells infected with different pestiviruses. J. Gen. Virol. **73:**47–52.
31. **Haller, O., G. Kochs, and F. Weber.** 2006. The interferon response circuit: induction and suppression by pathogenic viruses. Virology **344:**119–130.
32. **Heinz, F. X., M. S. Collett, R. H. Purcell, E. A. Gould, C. R. Howard, M. Houghton, R. J. M. Moormann, C. M. Rice, and H.-J. Thiel.** 2000. Family Flaviviridae, p. 859–878. *In* C. M. Fauquet, M. H. V. van Regenmortel, D. H. L. Bishop, E. B. Carstens, M. K. Estes, S. M. Lemon, J. Maniloff, M. A. Mayo, D. J. McGeoch, C. R. Pringle, and R. B. Wickner (ed.), Virus taxonomy. Seventh Report of the International Committee on Taxonomy of Viruses. Academic Press, San Diego, CA.
33. **Hilton, L., K. Moganeradj, G. Zhang, Y. H. Chen, R. E. Randall, J. W. McCauley, and S. Goodbourn.** 2006. The N^{pro} product of bovine viral diarrhea virus inhibits DNA binding by interferon regulatory factor 3 and targets it for proteasomal degradation. J. Virol. **80:**11723–11732.
34. **Hulst, M. M., F. E. Panoto, A. Hoekman, G. P. van Gennip, and R. J. M. Moormann.** 1998. Inactivation of the RNase activity of glycoprotein E^{rns} of classical swine fever virus results in a cytopathogenic virus. J. Virol. **72:**151–157.
35. **Kadowski, N., and Y. J. Liu.** 2002. Natural type 1 interferon-producing cells as a link between innate and adaptive immunity. Hum. Immunol. **63:**1126–1132.
36. **Kosmidou, A., M. Büttner, and G. Meyers.** 1998. Isolation and characterization of cytopathogenic classical swine fever virus (CSFV). Arch. Virol. **143:** 1295–1309.
37. **Kümmerer, B., D. Stoll, and G. Meyers.** 1998. Bovine viral diarrhea virus strain Oregon: a novel mechanism for processing of NS2-3 based on point mutations. J. Virol. **72:**4127–4138.
38. **Lackner, T., A. Mueller, M. Koenig, H.-J. Thiel, and N. Tautz.** 2005. Persistence of bovine viral diarrhea virus is determined by a cellular cofactor of a viral autoprotease. J. Virol. **79:**9746–9755.
39. **Lackner, T., A. Müller, A. Pankraz, P. Becher, H.-J. Thiel, A. E. Gorbalenya, and N. Tautz.** 2004. Temporal modulation of an autoprotease is crucial for replication and pathogenicity of an RNA virus. J. Virol. **78:**10765–10775.
40. **La Rocca, S. A., R. J. Herbert, H. Crooke, T. W. Drew, T. E. Wileman, and P. P. Powell.** 2005. Loss of interferon regulatory factor 3 in cells infected with classical swine fever virus involves the N-terminal protease, N^{pro}. J. Virol. **79:**7239–7247.
41. **Laude, H.** 1978. Isolation of a cytolytic strain of hog cholera virus from IB-RS2 cells. Ann. Microbiol. (Paris) **129:**553–561.
42. **Le Bon, A., and D. F. Tough.** 2002. Links between innate and adaptive immunity via type 1 interferon. Curr. Opin. Immunol. **14:**432–436.
43. **Lee, K. M., and J. H. Gillespie.** 1957. Propagation of virus diarrhea virus of cattle in tissue culture. Am. J. Vet. Res. **18:**953.
44. **Lindenbach, B. D., and C. M. Rice.** 2001. Flaviviridae: the viruses and their replication, p. 991–1041. *In* D. M. Knipe and P. M. Howley (ed.), Fields virology, 4th ed., vol. 1. Lippincott Williams & Wilkins, Philadelphia, PA.
45. **Mayer, D., M. A. Hofmann, and J. D. Tratschin.** 2004. Attenuation of classical swine fever virus by deletion of the viral N^{pro} gene. Vaccine **22:**317–328.
46. **Mendez, E., N. Ruggli, M. S. Collett, and C. M. Rice.** 1998. Infectious bovine viral diarrhea virus (strain NADL) RNA from stable cDNA clones: a cellular insert determines NS3 production and viral cytopathogenicity. J. Virol. **72:** 4737–4745.
47. **Meyers, G., T. Rümenapf, and H.-J. Thiel.** 1989. Ubiquitin in a togavirus. Nature **341:**491.
48. **Meyers, G., A. Saalmüller, and M. Büttner.** 1999. Mutations abrogating the RNase activity in glycoprotein E^{rns} of the pestivirus classical swine fever virus lead to virus attenuation. J. Virol. **73:**10224–10235.
49. **Meyers, G., D. Stoll, and M. Gunn.** 1998. Insertion of a sequence encoding light chain 3 of microtubule-associated proteins 1A and 1B in a pestivirus genome: connection with virus cytopathogenicity and induction of lethal disease in cattle. J. Virol. **72:**4139–4148.
50. **Meyers, G., N. Tautz, E. J. Dubovi, and H.-J. Thiel.** 1991. Viral cytopathogenicity correlated with integration of ubiquitin-coding sequences. Virology **180:**602–616.
51. **Meyers, G., and H.-J. Thiel.** 1995. Cytopathogenicity of classical swine fever virus caused by defective interfering particles. J. Virol. **69:**3683–3689.
52. **Meyers, G., and H.-J. Thiel.** 1996. Molecular characterization of pestiviruses. Adv. Virus Res. **47:**53–118.
53. **Mittelholzer, C., C. Moser, J.-D. Tratschin, and M. A. Hofmann.** 2000. Analysis of classical swine fever virus replication kinetics allows differentiation of highly virulent from avirulent strains. Vet. Microbiol. **74:**293–308.
54. **Moulin, H. R., T. Seuberlich, O. Bauhofer, L. C. Bennett, J. D. Tratschin, M. A. Hofmann, and N. Ruggli.** 2007. Nonstructural proteins NS2-3 and NS4A of classical swine fever virus: essential features for infectious particle formation. Virology **365:**376–389.
55. **Müller, A., G. Rinck, H. J. Thiel, and N. Tautz.** 2003. Cell-derived sequences in the N-terminal region of the polyprotein of a cytopathogenic pestivirus. J. Virol. **77:**10663–10669.
56. **Nagai, M., Y. Sakoda, M. Mori, M. Hayashi, H. Kida, and H. Akashi.** 2003. Insertion of cellular sequence and RNA recombination in the structural protein coding region of cytopathogenic bovine viral diarrhoea virus. J. Gen. Virol. **84:**447–452.
57. **Pocock, D. H., C. J. Howard, M. C. Clarke, and J. Brownlie.** 1987. Variation in the intracellular polypeptide profiles from different isolates of bovine viral diarrhea virus. Arch. Virol. **94:**43–53.

58. **Proletti, E., L. Bracci, S. Puzelli, T. Di Pucchio, P. Sestili, E. De Vincenzi, M. Venditti, I. Capone, I. Seif, E. De Maeyer, D. F. Tough, I. Donatelli, and F. Belardelli.** 2002. Type 1 IFN as a natural adjuvant for a protective immune response: lessons from the influenza vaccine model. J. Immunol. **169:**375–383.
59. **Rinck, G., C. Birghan, T. Harada, G. Meyers, H.-J. Thiel, and N. Tautz.** 2001. A cellular J-domain protein modulates polyprotein processing and cytopathogenicity of a pestivirus. J. Virol. **75:**9470–9482.
60. **Risatti, G. R., M. V. Borca, G. F. Kutish, Z. Lu, L. G. Holinka, R. A. French, E. R. Tulman, and D. L. Rock.** 2005. The E2 glycoprotein of classical swine fever virus is a virulence determinant in swine. J. Virol. **79:**3787–3796.
61. **Risatti, G. R., L. G. Holinka, C. Carillo, G. F. Kutish, Z. Lu, E. R. Tulman, I. F. Sainz, and M. V. Borca.** 2006. Identification of a novel virulence determinant within the E2 structural glycoprotein of classical swine fever virus. Virology **355:**94–101.
62. **Risatti, G. R., L. G. Holinka, I. Fernandez Sainz, C. Carrillo, Z. Lu, and M. V. Borca.** 2007. N-linked glycosylation status of classical swine fever virus strain Brescia E2 glycoprotein influences virulence in swine. J. Virol. **81:**924–933.
63. **Roehe, P. M., and S. Edwards.** 1994. Comparison of pestivirus multiplication in cells of different species. Res. Vet. Sci. **57:**210–214.
64. **Ruggli, N., B. H. Bird, L. Liu, O. Bauhofer, J. D. Tratschin, and M. A. Hofmann.** 2005. N(pro) of classical swine fever virus is an antagonist of double-stranded RNA-mediated apoptosis and IFN-alpha/beta induction. Virology **340:**265–276.
65. **Ruggli, N., J. D. Tratschin, M. Schweizer, K. C. McCullough, M. A. Hofmann, and A. Summerfield.** 2003. Classical swine fever virus interferes with cellular antiviral defense: evidence for a novel function of N^{pro}. J. Virol. **77:**7645–7654.
66. **Sainz, I. F., L. G. Holinka, Z. Lu, G. R. Risatti, and M. V. Borca.** 2008. Removal of a N-linked glycosylation site of classical swine fever virus strain Brescia E^{rns} glycoprotein affects virulence in swine. Virology **370:**122–129.
67. **Sakoda, Y., M. Hikawa, T. Tamura, and A. Fukusho.** 1998. Establishment of a serum-free culture cell line, CPK-NS, which is useful for assays of classical swine fever virus. J. Virol. Methods **75:**59–68.
68. **Schweizer, M., P. Mätzener, G. Pfaffen, H. Stalder, and E. Peterhans.** 2006. "Self" and "nonself" manipulation of interferon defense during persistent infection: bovine viral diarrhea virus resists alpha/beta interferon without blocking antiviral activity against unrelated viruses replicating in its host cells. J. Virol. **80:**6926–6935.
69. **Schweizer, M., and E. Peterhans.** 2001. Noncytopathic bovine viral diarrhea virus inhibits double-stranded RNA-induced apoptosis and interferon synthesis. J. Virol. **75:**4692–4698.
70. **Tautz, N., G. Meyers, R. Stark, E. J. Dubovi, and H.-J. Thiel.** 1996. Cytopathogenicity of a pestivirus correlated with a 27-nucleotide insertion. J. Virol. **70:**7851–7858.
71. **Tautz, N., G. Meyers, and H.-J. Thiel.** 1993. Processing of poly-ubiquitin in the polyprotein of an RNA virus. Virology **197:**74–85.
72. **Tautz, N., H.-J. Thiel, E. J. Dubovi, and G. Meyers.** 1994. Pathogenesis of mucosal disease: a cytopathogenic pestivirus generated by internal deletion. J. Virol. **68:**3289–3297.
73. **Thiel, H.-J., P. G. W. Plagemann, and V. Moennig.** 1996. Pestiviruses, p. 1059–1073. *In* B. N. Fields, D. M. Knipe, and P. M. Howley (ed.), Fields virology, 3rd ed., vol. 1. Lippincott-Raven Publishers, Philadelphia, PA.
74. **Tratschin, J.-D., C. Moser, N. Ruggli, and M. A. Hofmann.** 1998. Classical swine fever virus leader proteinase N^{pro} is not required for viral replication in cell culture. J. Virol. **72:**7681–7684.
75. **van Bekkum, J. G., and S. J. Barteling.** 1970. Plaque production by hog cholera virus. Arch. Gesamte. Virusforsch. **32:**185–200.
76. **Vassilev, V. B., and R. O. Donis.** 2000. Bovine viral diarrhea virus induced apoptosis correlates with increased intracellular viral RNA accumulation. Virus Res. **69:**95–107.
77. **von Wussow, P., D. Jakschies, H.-K. Hochkeppel, C. Fibich, L. Penner, and H. Deicher.** 1990. The human intracellular Mx-homologous protein is specifically induced by type 1 interferons. Eur. J. Immunol. **20:**2015–2019.
78. **Weiland, E., R. Ahl, R. Stark, F. Weiland, and H.-J. Thiel.** 1992. A second envelope glycoprotein mediates neutralization of a pestivirus, hog cholera virus. J. Virol. **66:**3677–3682.